Supplementary Information for

Atomic-Scale Structure and Local Chemistry of CoFeB-MgO Magnetic Tunnel Junctions

Zhongchang Wang,[†] Mitsuhiro Saito,[†,#] Keith P. McKenna,[‡,†] Shunsuke Fukami,[§,‖] Hideo Sato,[§,‖] Shoji Ikeda,[§,‖,⊥] Hideo Ohno,[†,§,‖,⊥] and Yuichi Ikuhara[†,#,▽]

[†]WPI Advanced Institute for Materials Research, Tohoku University, 2-1-1 Katahira, Aoba-ku, Sendai 980-8577, Japan

[‡]Department of Physics, University of York, Heslington, York YO10 5DD, UK

[§]Center for Spintronics Integrated Systems, Tohoku University, 2-1-1 Katahira, Aoba-ku, Sendai 980-8577, Japan

[‖]Center for Innovative Integrated Electronic Systems, Tohoku University, 468-1 Aramaki, Aza, Aoba-ku, Sendai 980-8577, Japan

[⊥]Laboratory for Nanoelectronics and Spintronics, Research Institute of Electrical Communication, Tohoku University, 2-1-1 Katahira, Aoba-ku, Sendai 980-8577, Japan

[#]Institute of Engineering Innovation, University of Tokyo, 2-11-16, Yayoi, Bunkyo-ku, Tokyo 113-8656, Japan

[▽]Nanostructures Research Laboratory, Japan Fine Ceramics Center, 2-4-1 Mutsuno, Atsuta, Nagoya 456-8587, Japan

Figure S1

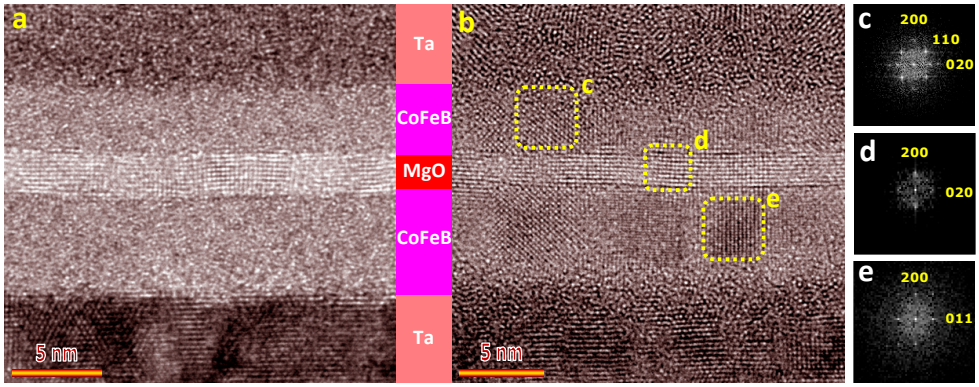

Figure S1. HRTEM imaging. Cs-corrected HRTEM images of (a) as-deposited and (b) annealed sample at 500^{o}C. Fast Fourier transformation (FFT) diffractograms obtained at a local region in (c) upper CoFe, (d) MgO tunnel barrier, and (e) lower CoFe in the annealed sample, as marked in (b).

Figure S2

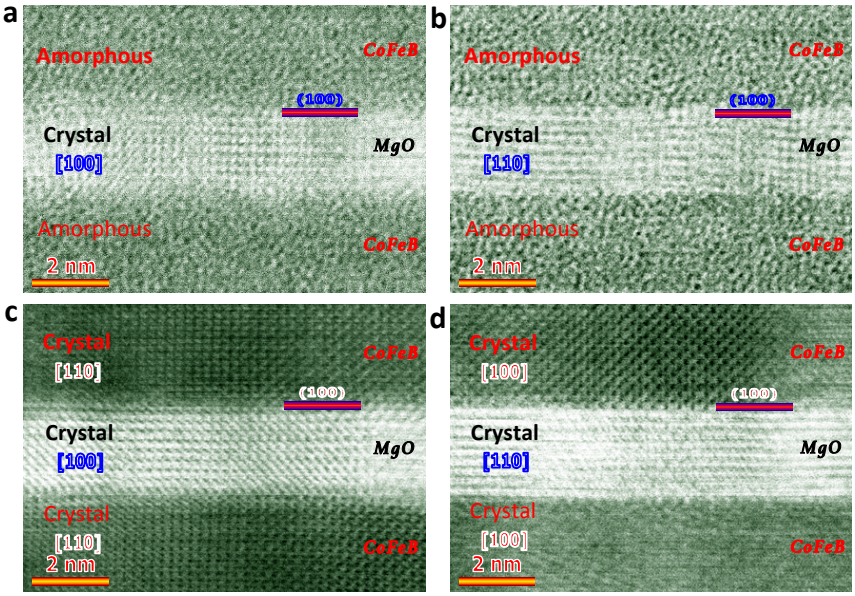

Figure S2. Structural transformation of the MTJ via annealing. ABF STEM images of the (a,b) as-deposited and (c,d) annealed samples taken from (a,c) [100] and (b,d) [110] direction of a nanocrystallite in MgO.

Figure S3

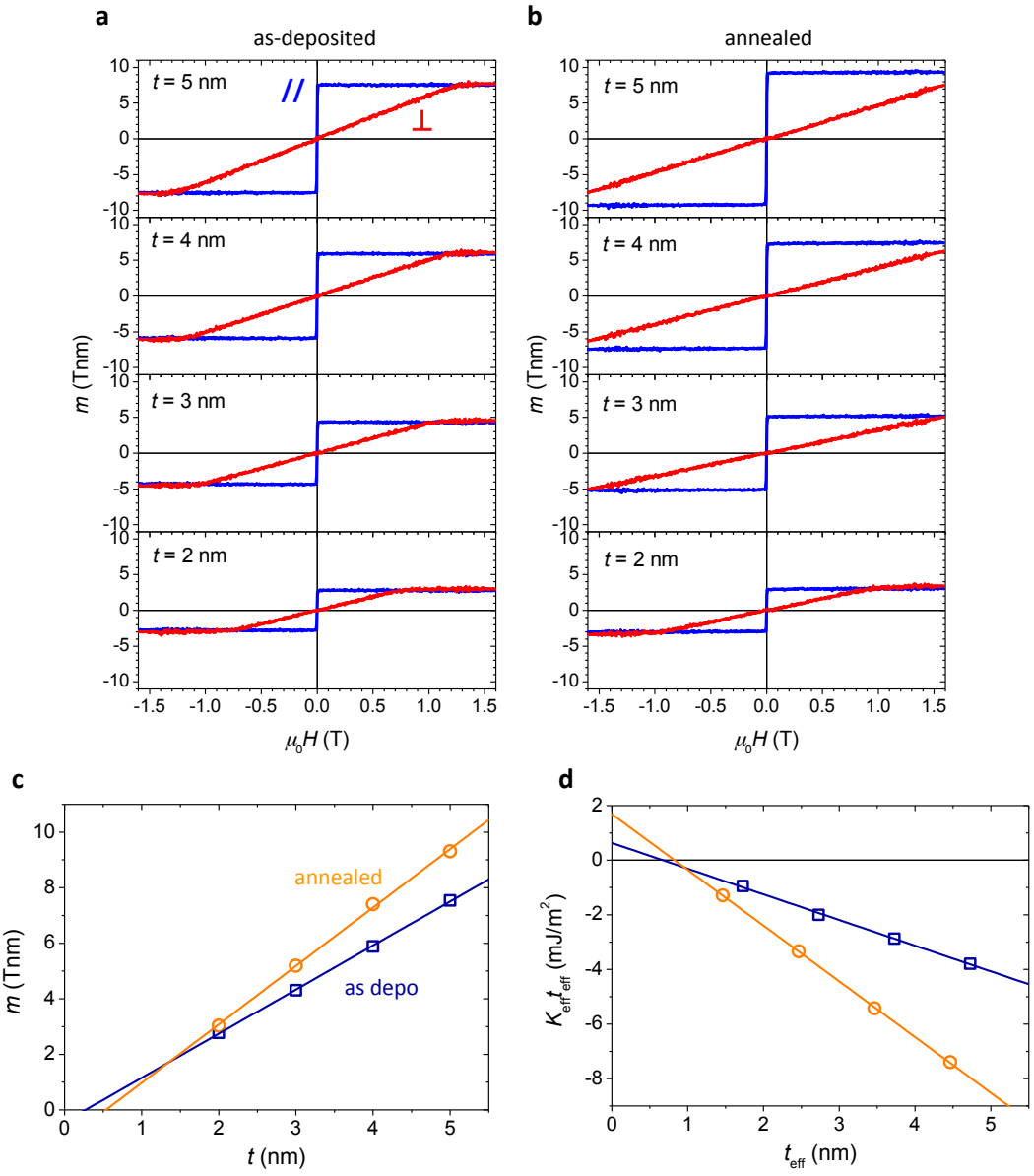

Figure S3. Magnetic properties. a,b, Hysteresis loops of CoFeB-MgO films with various CoFeB thickness t for (a) as-deposited and (b) annealed samples. (c) Magnetic moment per unit area m as a function of t. (d) Product of effective anisotropy K_{eff} and effective thickness t_{eff} as a function of effective CoFeB layer thickness.

Figure S4

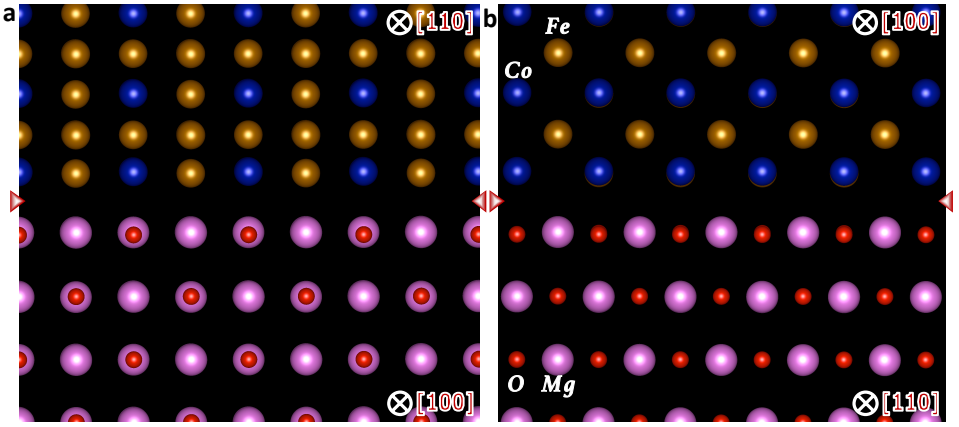

Figure S4. Relaxed atomic model of the CoFe/MgO interface. a,b, Relaxed model of the Fe_3Co/MgO interface viewed from the (a) [100] and (b) [110] direction of MgO. The Fe_3Co is adopted to represent the CoFe electrode. Location of the interface is indicated by arrows.

Figure S5

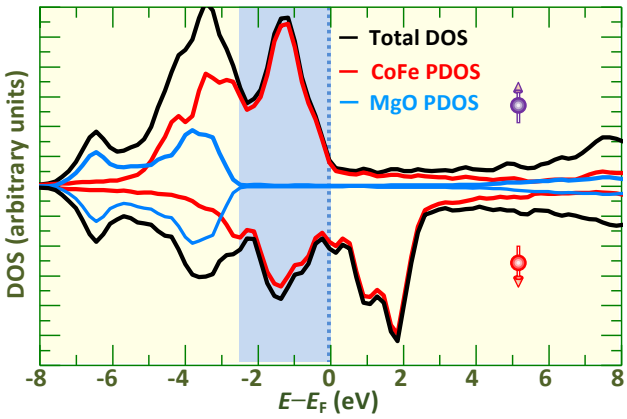

Figure S5. Electronic structure analysis. Total DOS and PDOS plots of CoFe and MgO contributions for the relaxed Fe_3Co/MgO interface. The interface atomic model is given in Figure S3. The Fermi level (E_F) is set to zero and marked by a dashed line.

Figure S6

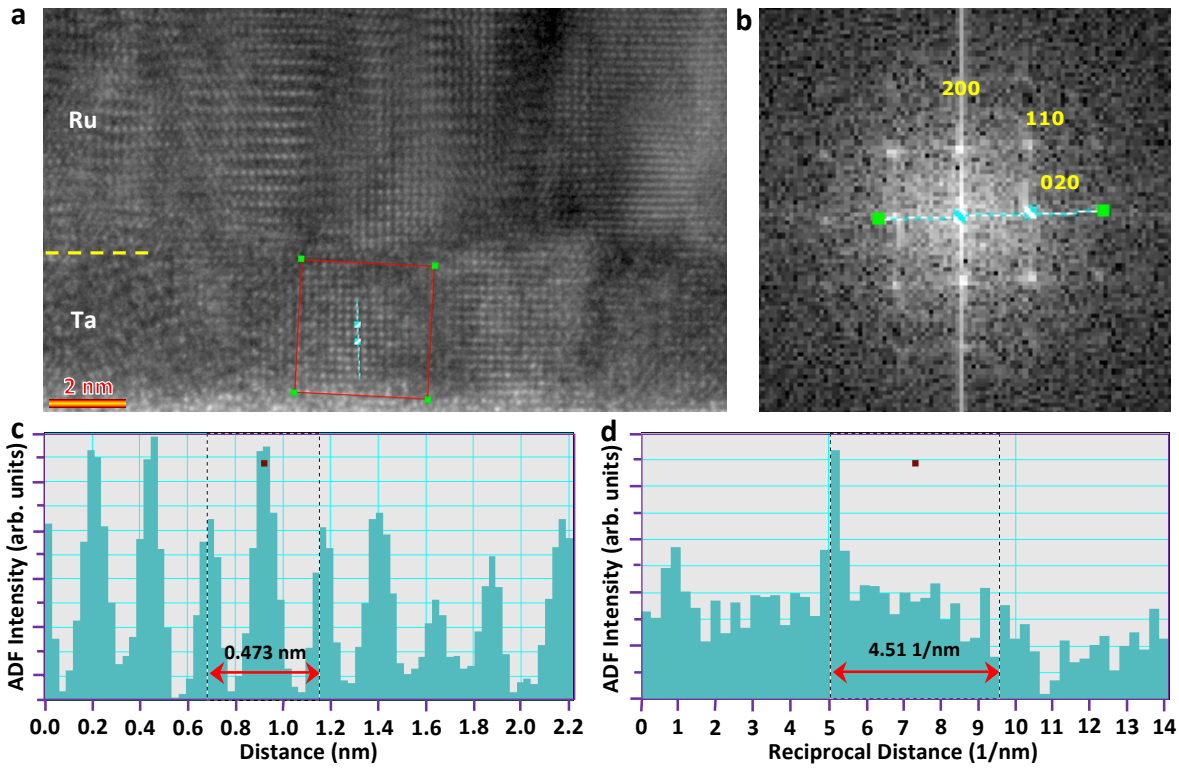

Figure S6. Structural analysis of nanocrystallites in Ta layer. (a) Cs-corrected HRTEM image of the Ta layer in the annealed sample. (b) Diffractogram obtained at a local region marked by a square in (a). (c) Line profile showing image intensity along the line marked in (a). (d) Line profile of the diffractogram showing intensity along the line marked in (b).

Table S1

Table S1. Summary of magnetic properties. Saturation magnetization M_s, magnetic dead layer thickness t_d, and interfacial magnetic anisotropy K_i for both the as-deposited and annealed samples, which are obtained based on the magnetization curves given in Fig. S3.

	As-deposited	Annealed
M_S (T)	1.59±0.02	2.10±0.05
t_d (nm)	0.27±0.05	0.54±0.08
K_i (mJ/m^2)	0.63±0.09	1.69±0.05

Supplementary Text

Measurement of magnetic properties

Magnetic properties of the samples used in the present TEM study are evaluated by measuring magnetization hysteresis loops using vibrating sample magnetometry. The stack structure is, from the substrate side, Ta(5)/Ru(10)/Ta(5)/CoFeB(t=2,3,4,5)/MgO(2.1)/CoFeB(0.4)/Ta(5)/Ru(5), where the numbers in the parentheses are nominal thickness in nm. To focus on the magnetic properties of the bottom CoFeB layer, the thickness of the top CoFeB layer is set to 0.4 nm, which has been found to show no magnetization signal due to its mixing with the top Ta layer.

Figure S3a,b shows the measured hysteresis loops along the in-plane and out-of-plane directions for both as-deposited and annealed films. Their saturation magnetic moment m_s as a function of nominal CoFeB thickness t is given in Figure S3c. The saturation magnetization M_s and magnetic dead layer thickness t_d are obtained based on slope and intercept on horizontal axis of the linear fit. Figure S3d shows the product of effective anisotropy energy density K_{eff} and effective magnetic layer thickness t_{eff} (= t – t_d) as a function of t_{eff}, where K_{eff} is determined from the areal difference between the out-of-plane and in-plane hysteresis loops. The interfacial anisotropy K_i is obtained from the intercept on vertical axis of the linear fit to $K_{eff}t_{eff}$ vs. t_{eff}. Table S1 summarizes the obtained M_s, t_d, and K_i for the as-deposited and annealed films. The M_s increases by a factor of 1.3 after annealing, which is consistent with the TEM observation showing that B atoms diffuse out of the CoFeB layer into the Ta layer. In addition, the K_i also increases by a factor of 2.7 as a consequence of annealing. This can be explained by

considering the formation of Fe(Co)-O bonds at the interface between CoFeB and MgO layers, which is known to be necessary for interfacial perpendicular anisotropy.

Interface construction

As mentioned in the main text, the orientation relationship between CoFe electrode and MgO is observed to be $(001)[100]_{MgO}||(001)[110]_{CoFe}$, based upon which the interface atomic model is established. The $L6_0$ (Ti_3Cu-type) ordered phase of the Fe_3Co, which is predicted as stable, is used to represent the CoFe electrodes. As for the stacking sequence, the interfacial Co/Fe atoms are located on top of the surface oxygen atoms of MgO based on the observed HAADF STEM image. The interface model is composed of a ten-layer $Fe_3Co(001)$ slab connected to a MgO(001) slab of six layers. A vacuum gap of 10 Å was included in the supercell to avoid the unwanted interaction between the slab and its periodic images. Along the interface plane, the two slabs utilize 1×1 cells, which are composed of a finite number of layers of infinite extent. To form a coherent interface, the in-plane lattice constants of Fe_3Co are expanded by 3.7% to match those of the harder MgO. The fully optimized atomic model of the interface is shown in Figure S4.

Adhesion energies of the interfaces

To shed light on which species of atom in CoFe electrodes is more favorable to bond MgO, we constructed two candidate models of Fe_3Co/MgO interface with two possible terminations: one where a 50% Co and 50% Fe plane is in contact with MgO, and the other with a 100% Fe in contact with MgO. We also constructed Co/MgO and Fe/MgO interface models as well for comparison. The *adhesion energy* W_{ad}, a key quantity in

predicting mechanical properties of an interface, is calculated by the difference in total energy between interface and its isolated slabs,

$$W_{ad} \equiv (E_{Fe_3Co} + E_{MgO} - E_{IF})/A, \quad (1)$$

where E_{Fe_3Co}, E_{MgO} and E_{IF} are total energies of the isolated Fe_3Co (Co or Fe) slab, MgO slab, and their interface, respectively, and A is interface area. The Fe_3Co/MgO interface terminated with 50% Co and 50% Fe exhibits a slightly larger W_{ad} than that terminated with 100% Fe by 0.1 J/m^2. In addition, W_{ad} of the Co/MgO interface is calculated to be 0.565 J/m^2, somewhat larger than that of the Fe/MgO interface (0.499 J/m^2). These results suggest that Co-terminated electrode is slightly more favorable to bond MgO than Fe-terminated one.

Analysis of structure of the nanocrystallites in the Ta Layer

To gain insights into structures of the nanocrystallites in the crystalline Ta layer, we conducted Cs-corrected HRTEM imaging and corresponding FFT diffractogram analysis of a Ta layer in the annealed sample, as shown in Figure S6. From Figure S6a, one can first confirm that the Ta layer is of crystalline nature with a textured structure. Further analysis of the diffractogram obtained at a local area of the Ta layer (marked by a square in Figure S6a) shows that the view direction is along [001] of Ta and the stacking plane is (110) (Figure S6b). Figure S6c shows the line profile of image intensity through a line marked in Figure S6a, revealing that lattice constant of the nanocrystallites in the Ta layer is ~3.32 Å (=4.47/√2 Å). This is further confirmed by the line profile on the diffractogram (Figure S6d) obtained through a line marked in Figure S6b, indicating that Ta nanocrystallites have the stable bcc structure (a = 3.306 Å).